Check for updates

ADVANCED ELECTRONIC MATERIALS
www.advelectronicmat.de

Peeling off Nanometer-Thick Ferromagnetic Layers and Their van der Waals Heterostructures

Kai Yuan, Xiaohan Yao, Hailong Wang, Bo Han, Peng Gao, Kenji Watanabe, Takashi Taniguchi, Lun Dai, Jianhua Zhao,* and Yu Ye**

The recent discovery of 2D van der Waals (vdWs) magnetic crystals provides an ideal platform for fundamental understanding of 2D magnetism, as well as the applications of low-power spintronic devices. One can integrate 2D magnetic materials into vdWs heterostructures with engineered properties, and also manipulate the magnetism via electrostatic gating. However, due to their instability, the handing of 2D magnetic materials can only be carried out under the help of encapsulation with other 2D materials (such as hexagonal boron nitride (*h*BN)) in a glove box, which is the biggest barrier toward its practical applications. Here, an approach about peeling-off and transfer of 2D ferromagnetic (Ga,Mn)As layers with thickness of ≈10–20 nm grown by the molecular beam epitaxy under ambient conditions is introduced. Transmission electron microscopy characterizations confirm the single-crystalline nature of the lifted-off (Ga,Mn)As. Superconducting quantum interference device measurements demonstrate that the lifted-off (Ga,Mn)As maintains its ferromagnetism. Using vdWs heterostructure assembly, technique *h*BN/(Ga,Mn)As top-gate Hall device and *p*-(Ga,Mn)As/*n*-MoS_2 heterojunction diode are fabricated. The electrical transport measurements demonstrate the ferromagnetic nature and gate tunable magnetoresistance of the lifted-off (Ga,Mn)As layer. This approach makes it possible to significantly expand the range of 2D ferromagnetic materials and their vdWs heterostructures.

Since the discovery of graphene in 2004,[1] the family of van der Waals (vdWs) materials has been growing rapidly, presenting a wide range of novel physical properties, such as semiconductors with spin-valley coupling,[2] Ising superconductors,[3] topological semimetals with edge transport[4] and Mott insulators with tunable charge-density waves,[5] etc. The recent addition of magnetic crystals in the two-dimensional (2D) material family, such as CrI_3, $Cr_2Ge_2Te_6$, and Fe_3GeTe_2, provides an ideal platform for fundamental understanding of 2D magnetism, as well as the applications of low-power spintronic devices.[6–8] The electrical control of 2D magnetic properties recently becomes possible, for example, conversion of bilayer CrI_3 from interlayer antiferromagnetism to ferromagnetism by electrostatic doping,[9,10] and electrical modulation of few-layer $Cr_2Ge_2Te_6$ coercivity and saturation field.[11] The advances of vdWs heterostructures can couple the quasiparticle interaction between the 2D magnetic material and others with engineered strain, chemistry, optical and electrical properties, providing an additional route to realize conceptual quantum phenomena and novel device functionalities, such as unprecedented control of the spin and

---

K. Yuan, X. Yao, Prof. L. Dai, Prof. Y. Ye
State Key Laboratory for Artificial Microstructure and Mesoscopic Physics and School of Physics
Peking University
Beijing 100871, China
E-mail: lundai@pku.edu.cn; ye_yu@pku.edu.cn

Prof. P. Gao, Prof. L. Dai, Prof. Y. Ye
Collaborative Innovation Center of Quantum Matter
Beijing 100871, China

Dr. H. Wang, Prof. J. Zhao
State Key Laboratory of Superlattices and Microstructures
Institute of Semiconductors
Chinese Academy of Sciences
Beijing 100083, China
E-mail: jhzhao@red.semi.ac.cn

The ORCID identification number(s) for the author(s) of this article can be found under https://doi.org/10.1002/aelm.201900345.

DOI: 10.1002/aelm.201900345

Prof. P. Gao
International Center for Quantum Materials
School of Physics
Peking University
Beijing 100871, China

B. Han, Prof. P. Gao
Electron Microscopy Laboratory
School of Physics
Peking University
Beijing 100871, China

B. Han
National Center for Materials Service Safety
University of Science and Technology Beijing
Beijing 100083, China

Dr. K. Watanabe, Dr. T. Taniguchi
National Institute for Materials Science
1-1 Namiki, Tsukuba 305-0044, Japan

valley pseudospin in WSe_2/CrI_3,[12] extremely large tunneling magnetoresistance based on graphene/GrI_3/graphene sandwich structures,[13,14] etc. Despite the intense efforts, a significant obstacle in realizing the promise of 2D magnetic materials is their instability under ambient conditions. Related work can only be carried out under the help of the encapsulation with other 2D materials (such as graphene and hexagonal boron nitride (*h*BN)) in a glove box.

(Ga,Mn)As, as representative dilute magnetic semiconductors, in which the presence of carriers promises the material to be a candidate for spintronic material.[15] In the past two decades, a variety of spintronic devices based on (Ga,Mn)As have been developed, such as gate-tunable ferromagnetism,[16] spin light-emitting diodes,[17] and magnetic tunnel junction,[18] etc. However, the synthesis of (Ga,Mn)As done using low-temperature molecular beam epitaxy (LT-MBE),[15,19] whereby (Ga,Mn)As is grown with atom layer precision on lattice-matched substrate, restricting its integration with some main-stream semiconductors, and flexible applications. By using an epitaxial lift-off (ELO) technique proposed by Yablonovitch et al.,[20] a 70 nm thick (Ga,Mn)As film has been lifted-off from the epitaxial substrate.[21] However, peeling off nanometer-thick (Ga,Mn)As layer and making its vdWs heterostructure device with other layered materials remain elusive. In this work, we introduce a method for lift-off thin (Ga,Mn)As films (≈10–20 nm) with size of hundreds of micrometers from the GaAs substrate, developed the deterministic dry transfer technique of lifted-off (Ga,Mn)As layer, and fabricated vdWs heterostructures based on the lifted-off (Ga,Mn)As. Transmission electron microscopy (TEM) characterizations confirmed the single-crystalline nature of the lifted-off (Ga,Mn)As. Superconducting quantum interference device (SQUID) magnetometer measurements demonstrated that the lifted-off sample maintained ferromagnetic order. Using the vdWs dry transfer method,[22] we fabricated *h*BN/(Ga,Mn)As top-gate Hall device and *p*-(Ga,Mn)As/*n*-MoS_2 heterojunction diode. Anomalous Hall effect and gate tunable magnetoresistance were observed in the low-temperature electrical transport measurements. The clear rectifying *I-V* curve of the *p-n* junction indicates the intact contact between the transferred (Ga,Mn)As and MoS_2. It is reasonable to envision that the ambient stable lifted-off ultrathin (Ga,Mn)As layer can be used as an alternative 2D magnetic materials, which could promote its applications, for example, on-chip low-power spintronics.

In order to realize epitaxial lift-off of the nanometer thick ferromagnetic (Ga,Mn)As layer from the lattice-matched substrate, a 1000-nm-thick $Al_{0.8}Ga_{0.2}As$ sacrificial layer was first grown on a GaAs substrate (step I in **Figure 1**a). Subsequently, a nanometer thick (10–20 nm) ferromagnetic $Ga_{0.94}Mn_{0.06}As$ layer was grown on the sacrificial layer via low-temperature MBE (step II in Figure 1a). Then, a thick layer of wax (Apiezon W) was spin-

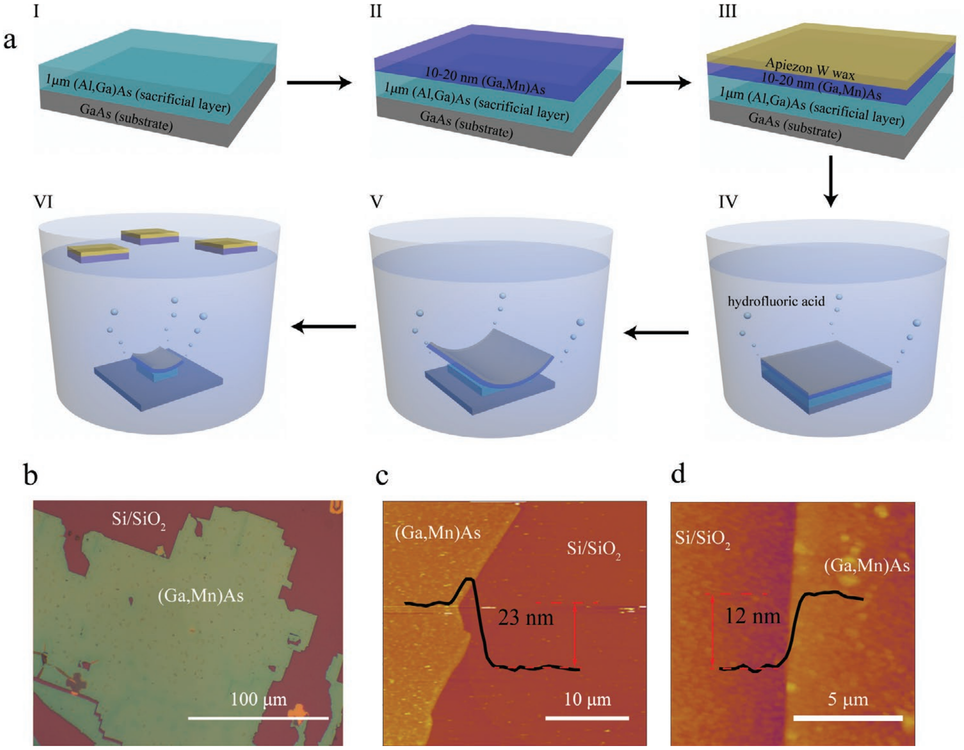

Figure 1. a) Schematic illustrations of peeling off nanometer thick (Ga,Mn)As film from MBE grown substrate. I, A 1000-nm-thick $Al_{0.8}Ga_{0.2}As$ sacrificial layer was first grown on a GaAs substrate by MBE. II, A 10–20 nm-thick ferromagnetic $Ga_{0.94}Mn_{0.06}As$ layer was grown on the sacrificial layer. III, A thick layer of wax (Apiezon W) was spincoated on the surface of (Ga,Mn)As as the supporting layer. IV, Hydrofluoric acid was used to separate the (Ga,Mn)As from the substrate by selectively etching the (Al,Ga)As sacrificial layer. V, $Al_{0.8}Ga_{0.2}As$ was etched away starting at the exposed edges and the (Ga,Mn)As layer was lifted off from the substrate. VI, The (Ga,Mn)As/Apiezon W films detached from the epitaxial substrate and floated on the top of the etchant. b) A typical optical image of lifted-off (Ga,Mn)As layer on a Si/SiO_2 substrate. c) The AFM image of a lifted-off 20 nm (Ga,Mn)As layer on a Si/SiO_2 substrate. d) The AFM image of a lifted-off 10 nm (Ga,Mn)As layer on a Si/SiO_2 substrate.

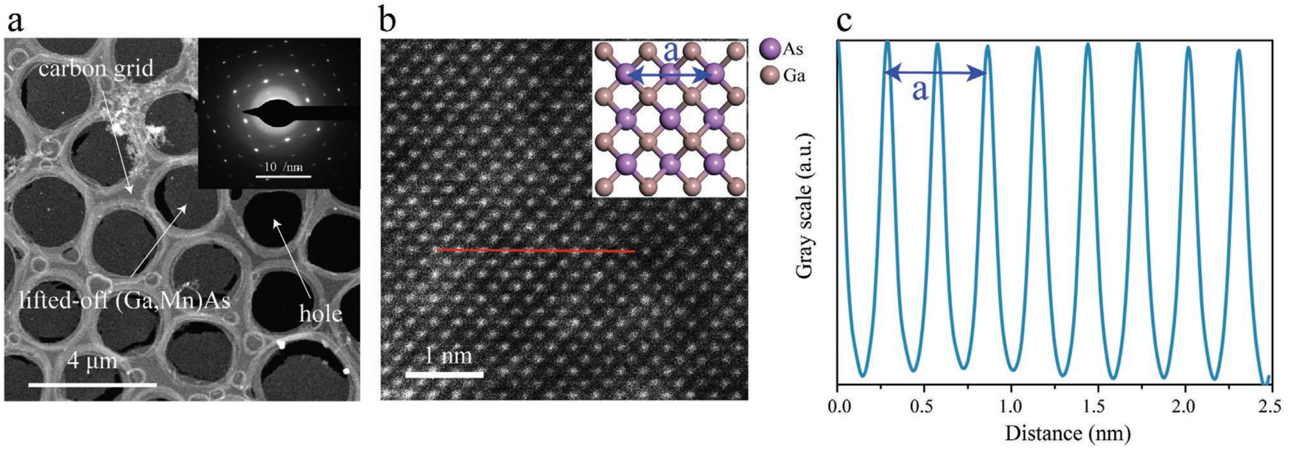

Figure 2. a) Large field-of-view HAADF-STEM image of a lifted-off 10 nm (Ga,Mn)As film. The inset is the corresponding SAED pattern, which confirms the high single-crystalline nature of the (Ga,Mn)As film. b) Atomic resolution HAADF-STEM image of the lifted-off (Ga,Mn)As film. The inset is the schematic diagram of the (001) crystal face of (Ga,Mn)As, in which the lattice constant (a) is indicated by the blue double-headed arrow line. c) The line profile (with smoothed intensity) of the HAADF-STEM image in (b) along the red line, from which the in-plane lattice constant is measured to be 0.577 nm.

coated onto the surface of (Ga,Mn)As as the supporting layer, which guarantees the integrity of the (Ga,Mn)As film (step III in Figure 1a). Apiezon W is a well-known etching resist, with the advantage of being inert to most acids (including HF) and easy removal after use.[20] After being baked at 100 °C for 30 min, 8% HF acid was used to separate the (Ga,Mn)As from the substrate by selectively etching away the (Al,Ga)As sacrificial layer (step IV in Figure 1a). Given the high etching selectivity between $Ga_{0.94}Mn_{0.06}As$ and $Al_{0.8}Ga_{0.2}As$ in diluted HF (1 to 10 million),[20] $Al_{0.8}Ga_{0.2}As$ was etched first from exposed edges (step V in Figure 1a). However, hydrogen (H_2) bubbles formed during the ELO process accumulated and rolled up the lifted (Ga,Mn)As layer, which are known to prevent further etching and even crack the supporting film into small pieces. After several hours, the (Ga,Mn)As/Apiezon W films gradually detached from the epitaxial substrate (step VI in Figure 1a), which was collected manually by Si chips and rinsed in deionized (DI) water at least three times. After that, the (Ga,Mn)As/Apiezon W film floating on the DI water was manually collected onto a Si/SiO_2 (285 nm) substrate and baked at 100 °C for 30 min. Finally, the Apiezon W was removed by trichloroethylene solution. The lifted-off and transferred (Ga,Mn)As layer maintains integrity over a scale of a few hundreds of micrometer (Figure 1b). Effectively removing the bubbles during the ELO process should avoid cracking of the film and result in a faster separation at a larger scale. The atomic force microscopy (AFM) height image of the lifted-off (Ga,Mn)As exhibits a nearly homogeneous color contrast, indicating the uniformity of sample thickness. The line profile shows a thickness of about 23 nm, agreeing well with the original thickness of the epitaxial (Ga,Mn)As layer (Figure 1c). Similarly, an approximately 12 nm thick (Ga,Mn)As layer was also successfully lifted-off and transferred onto the target substrate (Figure 1d). The lifted-off nanometer thick (Ga,Mn)As attached to the host substrate via the vdWs force. By employing the layer-by-layer assembly technique developed in 2D materials community,[22] the ferromagnetic (Ga,Mn)As layer could be integrated into the vdWs heterostructures with other 2D materials.

We evaluated the crystallinity of the epitaxial lifted-off (Ga,Mn)As flake using TEM, which is of great significance to understand its magnetic properties. Conventionally, preparing a TEM sample of MBE grown materials, one needs to go through the lengthy and precise processes of mechanical polishing and Ar ion milling, ensuring the sample is thin enough for electron beam to pass through.[23] Our above achievement drastically simplifies the TEM sample preparation process. We can easily transfer the lifted-off (Ga,Mn)As onto a copper microgrid (**Figure 2**a). The selected area electron diffraction (SAED) pattern (inset of Figure 2a) apparently shows one set of square spots, confirming the single-crystalline nature of the lifted-off (Ga,Mn)As. The high-angle annular dark-field scanning TEM (HAADF-STEM) image presents an apparent square structure (Figure 2b), which agrees well with the zinc blende structure of (Ga,Mn)As (inset of Figure 2b). The in-plane lattice constant of the (Ga,Mn)As film is measured to be ≈ 0.577 nm from the intensity profile (the corresponding inverse fast Fourier transform (iFFT) filtered image of Figure 2b was used for image smoothing) along the red line (Figure 2b,c), which is slightly larger than that of (001) crystal face of GaAs (≈0.565 nm). The experimental results are consistent with the theoretical predictions, where the lattice constant difference is ascribed to the point defects (Mn_{Ga} and Mn_I) in the (Ga,Mn)As.[19,24]

The magnetic properties of the lifted-off (Ga,Mn)As layer are essential to integrate it into vdWs heterostructures with other 2D materials for spintronic devices. We employed SQUID magnetometer measurements to characterize the magnetic behavior of a 20 nm (Ga,Mn)As layer before and after lift-off. The magnetic moment (*M*) dependence of the magnetic field applied parallel to the as-grown 20 nm (Ga,Mn)As epitaxial layer (*M*-*H* curve, **Figure 3**a) exhibits a clear hysteresis loop with a coercivity field of ≈80 Oe (inset of Figure 3a), indicating the presence of ferromagnetic order. The *M*-*T* curve measured at 20 Oe (Figure 3b) shows that the Curie temperature (T_C) of the as-grown (Ga,Mn)As is about 90 K (Figure 3b). The *M*-*H* curve of the lifted-off (Ga,Mn)As demonstrates the maintained ferromagnetic order (Figure 3c) with an increased coercivity

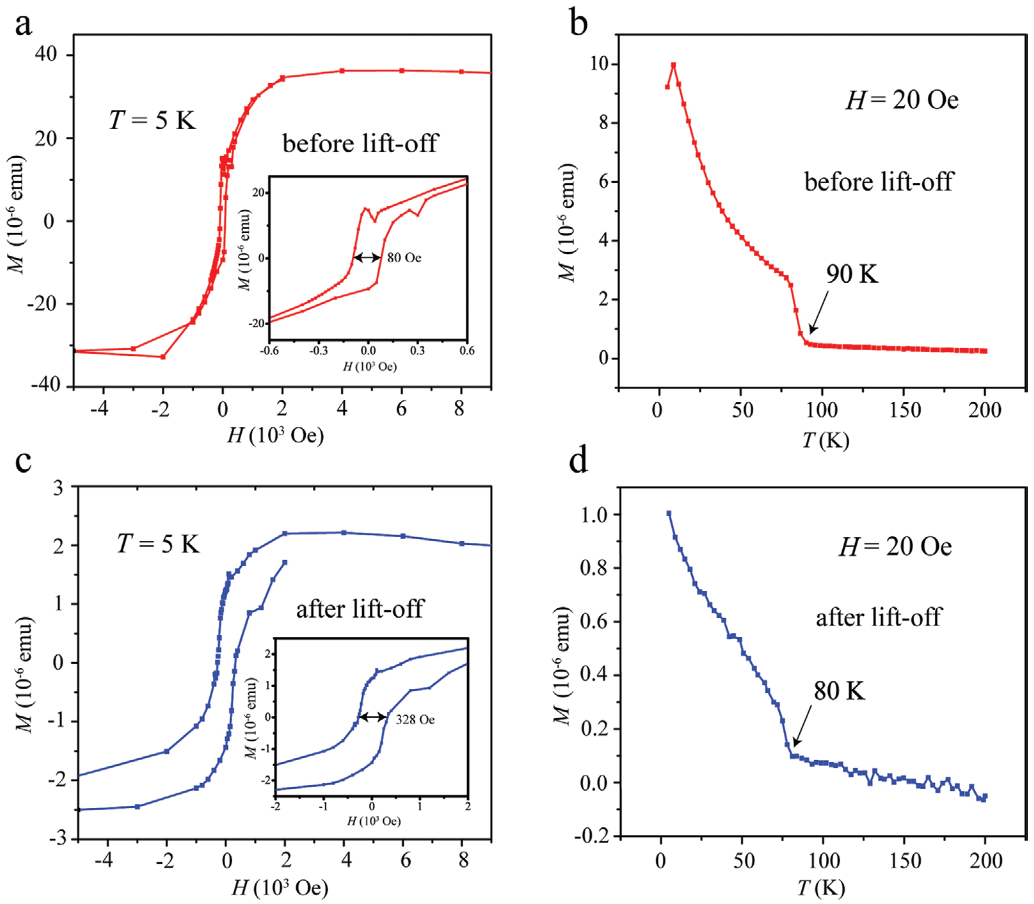

Figure 3. a) The *M-H* curve of the as-grown (Ga,Mn)As film before lift-off at 5 K. b) The *M-T* curve of the as-grown (Ga,Mn)As film before lift-off. c) The *M-H* curve of (Ga,Mn)As film after lift-off at 5 K. d) The *M-T* curve of the (Ga,Mn)As film after lift-off.

field of ≈328 Oe (inset of Figure 3c), which may stem from the enhanced magnetic anisotropy through releasing the growth-induced strain in (Ga,Mn)As layer and/or the decrease of the number of magnetic domains reducing the film size.[25,26] T_C of the lifted-off (Ga,Mn)As is measured to be about 80 K (Figure 3d), slightly lower than that of the as-grown (Ga,Mn)As. These results clearly demonstrated that the (Ga,Mn)As layer maintained its ferromagnetic properties after lift-off.

Researchers have long been desiring to control the magnetic properties of (Ga,Mn)As by external electrical field, as (Ga,Mn)As layer exhibits carrier-mediated ferromagnetism.[16,19] The lifted-off ultrathin (Ga,Mn)As layer makes this easy to be realized. To demonstrate this, we constructed a *h*BN/(Ga,Mn)As top-gated Hall device (**Figure** 4a). Pd/Au (10 nm/40 nm) ohmic contact electrodes with Hall-bar structure were fabricated by electron-beam lithography on a lifted-off 20 nm rectangle-shaped (Ga,Mn)As flake transferred on a Si/SiO$_2$ substrate. Then, a piece of *h*BN (≈20 nm) was transferred onto the Hall device as the top gate dielectric layer via the dry transfer method. Subsequently, the top-gate electrode was defined by a similar metallization process. The channel current decreases with increasing top-gate voltage (V_g), indicating the *p*-type nature of the (Ga,Mn)As. The channel cannot be fully depleted by the top-gate voltage of up to 6 V (Figure 4b), indicating the heavily *p*-type doped nature of the (Ga,Mn)As. The hole concentration (p) is estimated to be ≈ 3.92×10^{20} cm^{-3}. The temperature dependence of the longitudinal resistance of the lifted-off (Ga,Mn)As layer, R_{xx}, was measured from 2 to 300 K (Figure 4c). A local maximum of R_{xx}, which corresponds to T_C (i.e., the para- to ferromagnetic phase transition temperature), was observed near 90 K. When the temperature is below T_C, the R_{xx} decreases with T decreasing. This is because spin-flip scattering decreases when stronger ferromagnetism is established.[27,28] A resistivity minimum is observed with a corresponding temperature, T_M, around 15 K, which may be associated with Kondo effect arising from the existence of Mn interstitials in the (Ga,Mn)As layer.[29] The observation verified again the high quality of the lifted-off layer.

The out-of-plane magnetic field (B) sweeps of R_{xx} at different temperatures are shown in Figure 4d. At low temperature, the resistance shows two distinct peaks resulting from the anisotropic magnetoresistance (AMR), that is, positive MR at small B, and negative MR at high B. The negative MR is associated with the strong alignment of spins at high B, which suppresses spin disorder.[30] As the temperature increases, the twin AMR peaks decrease, and disappear at temperatures higher than T_C. In our case, we can easily modulate the MR by gate voltage. Besides changing the absolute resistance values, the slopes of the negative MR became sharper with application of positive back-gate voltages (V_{bg}) measure at 10 K (Figure 4e). This is because that,

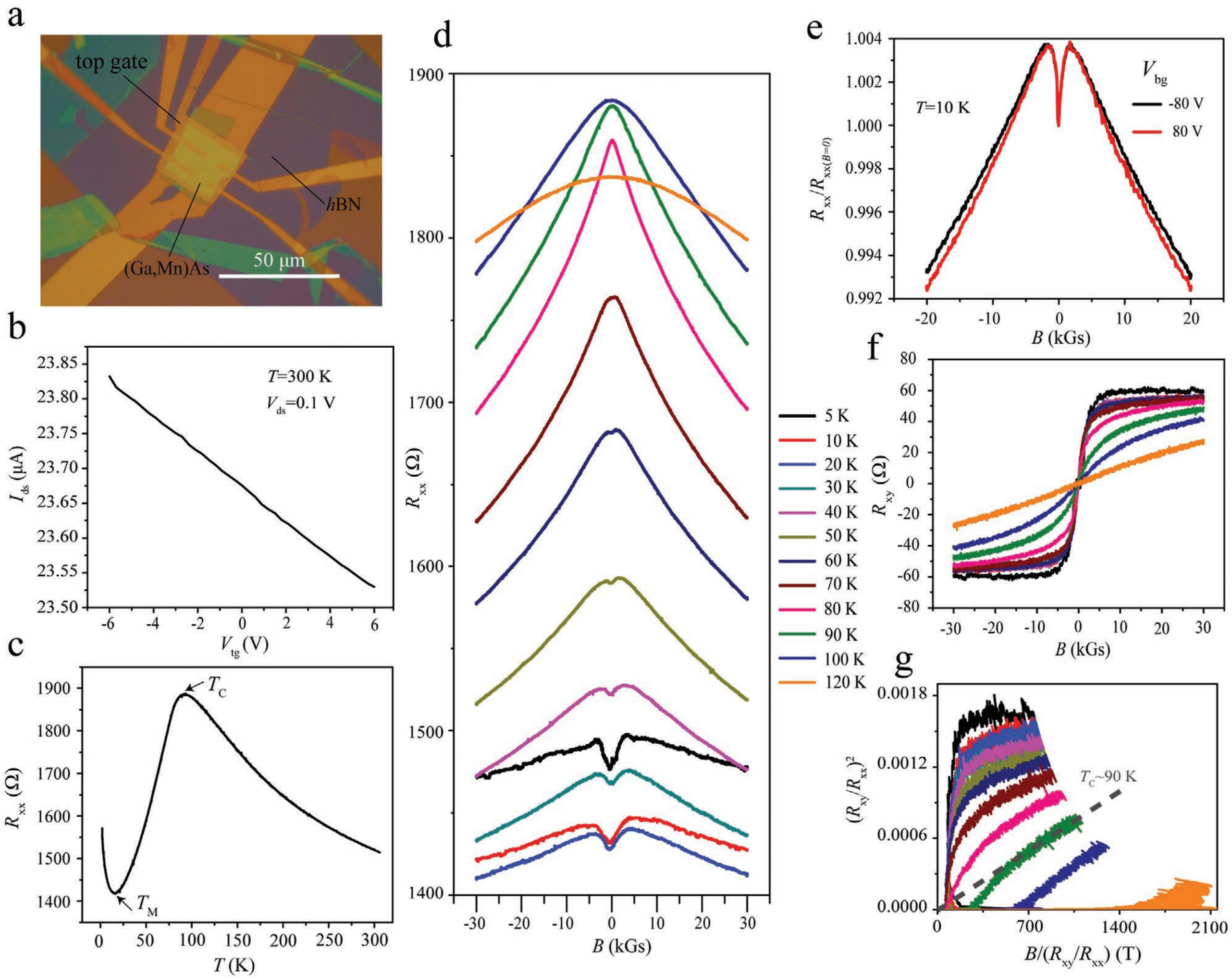

Figure 4. a) The optical image of a typical *h*BN/(Ga,Mn)As top-gate Hall device. b) Top-gate transfer curve of the lifted-off (Ga,Mn)As layer, showing a clear *p*-type behavior. c) Temperature dependence of the longitudinal resistance of the lifted-off (Ga,Mn)As layer. d) Out-of-plane magnetic field sweeps of R_{xx} of the lifted-off (Ga,Mn)As layer at different temperatures. e) In-plane magnetic field sweeps of R_{xx} of the lifted-off (Ga,Mn)As layer at 10 K with different back-gate voltage. f) Out-of-plane magnetic field sweeps of R_{xy} of the lifted-off (Ga,Mn)As layer at different temperatures. g) The Arrott plot of the lifted-off (Ga,Mn)As layer. The magnetic transition temperature of ≈90 K was determined.

for the hole-mediated ferromagnetic semiconductor, depletion (under positive V_{bg}) would de-stabilize the coupling between Mn magnetic moments, in contrast to the case under negative V_{bg} (which causes hole accumulation).[31] Under this circumstance, the applied magnetic field (0.5–2 T) would align Mn moments more at positive V_{bg}, resulting in larger negative MR slopes. The observed saturated curves of R_{xy} versus out-of-plane B at temperatures below T_C signify the anomalous Hall effect (Figure 4f), which is a typical phenomenon in ferromagnetic semiconductors.[15,19] In the Arrott plot (Figure 4g), where $(R_{xy}/R_{xx})^2$ is plotted versus $B/(R_{xy}/R_{xx})$, the transition temperature at which the sample magnetization crosses the origin at zero applied B is determined to be ≈90 K[32] (gray dashed line in Figure 4g), agreeing well with the Curie temperature determined by above electrical transport measurements.

Given the successful lift-off of the nanometer thick (Ga,Mn)As layer and its high stability in ambient condition, the integration of (Ga,Mn)As layer with other 2D materials through noncovalent interactions extends the research scope and progress of ferromagnetic vdW heterostructures. For example, we assembled a vdWs heterostructure with lifted-off *p*-type (Ga,Mn)As layer and exfoliated *n*-type few-layer MoS_2 using the dry transfer method (**Figure 5**a). First, we picked up previously lifted-off (Ga,Mn)As layer from Si/SiO_2 substrate by a poly dimethylsiloxane (PDMS) stamp covered by a layer of polypropylene carbonate (PPC) with the help of a glass slide (step I in Figure 5b) in ambient. After that, we put the PPC with (Ga,Mn)As facing down onto the exfoliated MoS_2 flake (step II in Figure 5b) and left it on the MoS_2 to form the vdWs heterostructure (step III in Figure 5b). The Ti/Au (5/20 nm) electrodes were defined on (Ga,Mn)As and MoS_2 regions, respectively. The back-gate voltage transfer curve of the MoS_2 flake exhibits *n*-type behavior with a turn-on voltage around −10 V and on-off current ratio of ≈10^7 (black curve in Figure 5c). The transfer curve of the (Ga,Mn)As exhibits heavily doped *p*-type behavior (red curve in Figure 5c). The *I*-*V* characteristic of

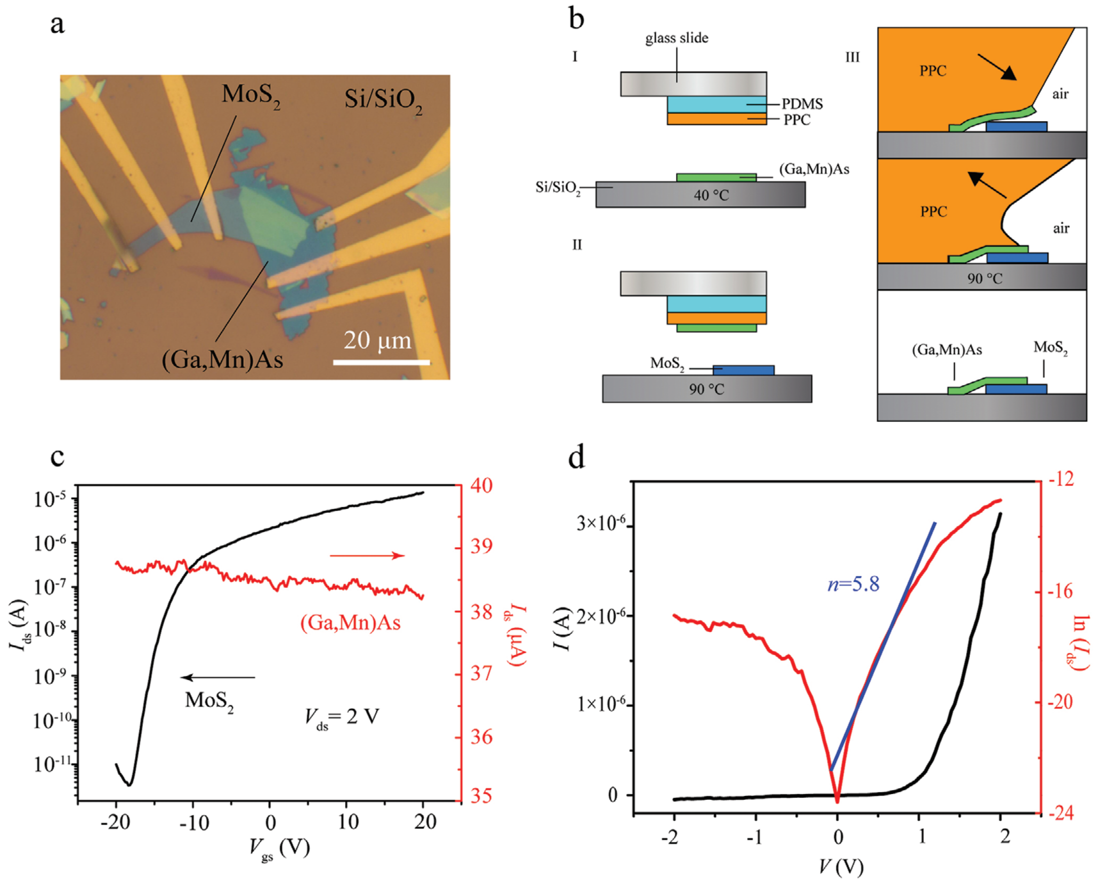

Figure 5. a) The optical image of a typical p-(Ga,Mn)As/n-MoS_2 heterojunction diode. b) The schematic diagrams of the dry transfer method to assemble the p-(Ga,Mn)As/n-MoS_2 vdWs heterostructure. c) The back gate voltage dependent transfer curves of the MoS_2 flake (black) and the (Ga,Mn)As layer (red), respectively. d) Room-temperature I-V characteristics of the p-(Ga,Mn)As/n-MoS_2 heterojunction diode in linear scale (black) and semi-log scale (red), respectively. The blue line shows the curve fitting result with an ideality factor n of about 5.8.

the (Ga, Mn)As/MoS_2 vdWs heterojunction shows a clear rectifying behavior when the voltage changes from −2 to 2 V, with a rectification ratio of 10^2 (Figure 5d). The turn on voltage is ≈1 V. The I-V relationship of a p-n junction can be expressed as $I = I_0\,[\exp(qV/nkT)\text{-}1]$, where I_0 is the reverse saturation current, k is the Boltzmann constant, T is the temperature, q is the electron charge, and n is the ideality factor. By fitting the measured I-V curve, $n = 5.8$ can be obtained. These results infer that we are able to integrate the lifted-off (Ga,Mn)As with other 2D material with different physical properties into vdWs heterostructures using the developed lift-off and transfer method of the (Ga,Mn)As layer under ambient condition, which may open a new route for novel vdWs spintronic devices.

In summary, we successfully peeled-off 2D (Ga,Mn)As of 10–20 nm with sizes of hundreds of micrometers from the MBE-grown substrates, developed the deterministic dry transfer, and fabricated hBN/(Ga,Mn)As top-gate Hall device and p-(Ga,Mn)As/n-MoS_2 heterojunction diode. The HAADF-STEM characterizations confirmed the single-crystalline nature of the 2D (Ga,Mn)As. The SQUID magnetometer measurements, as well as the electrical transport measurements, demonstrated the maintained ferromagnetic order. The gate tunable magnetoresistance and rectification characteristic were observed in the top-gate Hall device and pn heterojunction, respectively. Our achievement helps to expand the 2D ferromagnetic material system and related vdWs heterostructures, which benefits in exploring novel physical properties and diverse device functionality under ambient condition, such as on-chip low-power spintronics devices etc.

Experimental Section

vdWs Transfer Method: The dry transfer method is described by assembling p-(Ga,Mn)As/n-MoS_2 vdWs heterojunction layer-by-layer as an example. A piece of adhesive tape with a hole in the center was first adhered to a Si chip. Then, the Si chip was coated with PPC (Sigma-Aldrich, CAS 25 511-85-7) at 2000 rpm. The tape with a PPC thin film was manually peeled from the Si substrate and placed onto a transparent elastomer stamp (PDMS, Gel-Pak PF-40/17-X4) affixed on a glass slide. The glass slide with the PDMS stamp was flipped and attached to a micromanipulator with the PPC film side down. In parallel, the lifted-off 20 nm (Ga,Mn)As layers were transferred onto a Si/SiO_2 (285 nm) substrate, which was placed onto a heating plate under an optical microscope. The micromanipulator was used to align the PPC with the chosen (Ga,Mn)As layer and bring them into contact. When the heating plate temperature was set at 40 °C, the (Ga,Mn)As layer would adhere more strongly to the PPC than to the Si/SiO_2 and could be lifted off from the substrate. After that, the PPC with the (Ga,Mn)As layer was aligned to contact a chosen n-MoS_2 flake (10–30 nm thick) exfoliated on another Si/SiO_2 substrate. Under 90 °C heating plate temperature, the PPC began to melt, and the (Ga,Mn)As layer adhered more strongly to the MoS_2 flake and Si/SiO_2 substrate than to the PPC. Then, the PPC was removed by acetone. Thus, the *p*-(Ga,Mn)As/*n*-MoS_2 vdWs heterojunction was obtained on the device substrate. In order to assemble the *h*BN/(Ga,Mn)As top-gate Hall device, a similar dry transfer process was performed.

Atomic Force Microscopy Characterization: AFM measurements were carried out with an atomic force microscope (Cypher S, Asylum Research) under ambient condition using tapping mode.

Transmission Electron Microscopy Characterization: SAED and STEM measurements were carried out by an aberration-corrected Titan Themis G2 microscope at 300 kV with a beam current of 50 pA.

Electrical Transport Measurements: The device electrical transport measurements were performed in a superconducting magnet system (model c-mag vary-14 T research system by Cryomagnetics).

Acknowledgements

This work was supported by the National Key R&D Program of China (Grant Nos. 2017YFA0206301 and 2018YFA0306900), National Natural Science Foundation of China (Nos. 61521004, 61874003, 11474007, and U1632264), and Beijing Natural Science Foundation (4182028). K.W. and T.T. acknowledge support from the Elemental Strategy Initiative conducted by the MEXT, Japan, A3 Foresight by JSPS and the CREST (JPMJCR15F3), JST. The authors thank Shuang Jia for the help in sealing the ampules. The authors acknowledge Electron Microscopy Laboratory in Peking University for the use of Cs corrected electron microscope.

Conflict of Interest

The authors declare no conflict of interest.

Keywords

(Ga, Mn)As, lift-off, transfer, 2D magnetism, van der Waals heterostructure

Received: April 4, 2019
Revised: July 9, 2019
Published online: July 30, 2019

---

[1] K. S. Novoselov, A. K. Geim, S. V. Morozov, D. Jiang, Y. Zhang, S. V. Dubonos, I. V. Grigorieva, A. A. Firsov, *Science* **2004**, *306*, 666.
[2] X. Xu, W. Yao, D. Xiao, T. F. Heinz, *Nat. Phys.* **2014**, *10*, 343.
[3] J. M. Lu, O. Zheliuk, I. Leermakers, N. F. Q. Yuan, U. Zeitler, K. T. Law, J. T. Ye, *Science* **2015**, *350*, 1353.
[4] X. Qian, J. Liu, L. Fu, J. Li, *Science* **2014**, *346*, 1344.
[5] Y. Yu, F. Yang, X. F. Lu, Y. J. Yan, Y. Cho, L. Ma, X. Niu, S. Kim, Y. Son, D. Feng, S. Li, S. Cheong, X. Chen, Y. Zhang, *Nat. Nanotechnol.* **2015**, *10*, 270.
[6] B. Huang, G. Clark, E. N. Moratalla, D. R. Klein, R. Cheng, K. L. Seyler, D. Zhong, E. Schmidgall, M. A. McGuire, D. H. Cobden, W. Yao, D. Xiao, P. J. Herrero, X. Xu, *Nature* **2017**, *546*, 270.
[7] C. Gong, L. Li, Z. Li, H. Ji, A. Stern, Y. Xia, T. Cao, W. Bao, C. Wang, Y. Wang, Z. Q. Qiu, R. J. Cava, S. G. Louie, J. Xia, X. Zhang, *Nature* **2017**, *546*, 265.
[8] Y. Deng, Y. Yu, Y. Song, J. Zhang, N. Z. Wang, Z. Sun, Y. Yi, Y. Z. Wu, S. Wu, J. Zhu, J. Wang, X. H. Chen, Y. Zhang, *Nature* **2018**, *563*, 94.
[9] S. Jiang, L. Li, Z. Wang, K. F. Mak, J. Shan, *Nat. Nanotechnol.* **2018**, *13*, 549.
[10] B. Huang, G. Clark, D. R. Klein, D. MacNeill, E. N. Moratalla, K. L. Seyler, N. Wilson, M. A. McGuire, D. H. Cobden, D. Xiao, W. Yao, P. J. Herrero, X. Xu, *Nat. Nanotechnol.* **2018**, *13*, 544.
[11] Z. Wang, T. Zhang, M. Ding, B. Dong, Y. Li, M. Chen, X. Li, J. Huang, H. Wang, X. Zhao, Y. Li, D. Li, C. Jia, L. Sun, H. Guo, Y. Ye, D. Sun, Y. Chen, T. Yang, J. Zhang, S. Ono, Z. Han, Z. Zhang, *Nat. Nanotechnol.* **2018**, *13*, 554.
[12] K. L. Seyler, D. Zhong, B. Huang, X. Linpeng, N. P. Wilson, T. Taniguchi, K. Watanabe, W. Yao, D. Xiao, M. A. McGuire, K. C. Fu, X. Xu, *Nano Lett.* **2018**, *18*, 3823.
[13] T. Song, X. Cai, M. W. Tu, X. Zhang, B. Huang, N. P. Wilson, K. L. Seyler, L. Zhu, T. Taniguchi, K. Watanabe, M. A. McGuire, D. H. Cobden, D. Xiao, W. Yao, X. Xu, *Science* **2018**, *360*, 1214.
[14] D. R. Klein, M. MacNeill, J. L. Lado, D. Sorinao, E. Navarro-Moratalla, K. Watanabe, T. Taniguchi, S. Manni, P. Canfield, J. Fernández-Rossier, P. Jarillo-Herrero, *Science* **2018**, *360*, 1218.
[15] H. Ohnoa, A. Shen, F. Matsukura, A. Oiwa, A. Endo, S. Katsumoto, Y. Iye, *Appl. Phys. Lett.* **1996**, *69*, 363.
[16] D. Chiba, F. Matsukura, H. Ohno, *Appl. Phys. Lett.* **2006**, *89*, 162505.
[17] Y. Ohno, D. K. Young, B. Beschoten, F. Matsukura, H. Ohno, D. D. Awschalom, *Nature* **1999**, *402*, 790.
[18] M. Tanaka, Y. Higo, *Phys. Rev. Lett.* **2001**, *87*, 026602.
[19] H. Ohno, *Science* **1998**, *281*, 951.
[20] E. Yablonovitch, T. Gmltter, J. P. Harbison, R. Bhat, *Appl. Phys. Lett.* **1987**, *51*, 2222.
[21] F. Greulleta, L. Ebel, F. Münzhuber, S. Mark, G. V. Astakhov, T. Kießling, C. Schumacher, C. Gould, K. Brunner, W. Ossau, L. W. Molenkamp, *Appl. Phys. Lett.* **2011**, *98*, 231903.
[22] L. Wang, I. Meric, P. Y. Huang, Q. Gao, Y. Gao, H. Tran, T. Taniguchi, K. Watanabe, L. M. Campos, D. A. Muller, J. Guo, P. Kim, J. Hone, K. L. Shepard, C. R. Dean, *Science* **2013**, *342*, 614.
[23] A. Kovács1, J. Sadowski, T. Kasama, J. Domagała, R. Mathieu, T. Dietl, R. E. Dunin-Borkowski, *J. Appl. Phys.* **2011**, *109*, 083546.
[24] J. Mašek, J. Kudrnovský, F. Máca, *Phys. Rev. B.* **2003**, *67*, 153203.
[25] F. Matsukura, M. Sawicki, T. Dietl, D. Chiba, H. Ohno, *Phys. E* **2004**, *21*, 1032.
[26] M. Glunk, J. Daeubler, L. Dreher, S. Schwaiger, W. Schoch, R. Sauer, W. Limmer, A. Brandlmaier, S. T. B. Goennenwein, C. Bihler, M. S. Brandt, *Phys. Rev. B.* **2009**, *79*, 195206.
[27] T. Hayashi, Y. Hashimoto, S. Katsumoto, Y. Iyea, *Appl. Phys. Lett.* **2001**, *78*, 1691.
[28] K. W. Edmonds, K. Y. Wang, R. P. Campion, A. C. Neumann, N. R. S. Farley, B. L. Gallagher, C. T. Foxon, *Appl. Phys. Lett.* **2002**, *81*, 4991.
[29] H. T. He, C. L. Yang, W. K. Ge, J. N. Wang, *Appl. Phys. Lett.* **2005**, *87*, 162506.
[30] T. Omiya, F. Matsukura, T. Dietl, Y, Ohno , T. Sakon, M. Motokawa, H. Ohno, *Phys. E* **2000**, *7*, 976.
[31] M. H. S. Owen, *Doctoral Dissertation*, University of Cambridge **2010**.
[32] I. Yeung, R. M. Roshko, G. Williams, *Phys. Rev. B.* **1986**, *34*, 3456.